2024, 21(12): 3661-3672
https://doi.org/10.21123/bsj.2024.9852
P-ISSN: 2078-8665 - E-ISSN: 2411-7986
Baghdad Science Journal

Syntheses, Characterisation, Thermal Analysis and Theoretical Studies of Some Imino Ethanone Metal Complexes

Safaa H. Ali*[1], Saad S. Mohammed[2] Hadi T. Obaid[3], Sanjeewa Gamagedara[4]

[1]Department of Chemistry and Physiological, College of Veterinary Medicine, Al-Shatrah University, Al-Shatrah, Iraq.
[2]Department of Chemistry, College of Science, University of Thi-Qar, Al-Nasyriah, Iraq.
[3]Department of Physics, College of Applied Science, Al-Shatrah University, Al-Shatrah, Iraq.
[4]Department of Chemistry, College of Mathematics and Science, University of Central Oklahoma, Edmond, Oklahoma, USA.
*Corresponding Author

Received 05/10/2023, Revised 09/02/2024, Accepted 11/02/2024, Published Online First 20/05/2024, Published 01/12/2024

Abstract

The current study is designed to synthesize four new bidentate metal complexes [MCl_2L1] M = Co, Cu and L1 = 1,2-Diphenyl-2-(phenylimino)-1-ethanone or [MCl_2L2] M = Co, Cu and L2 = 1,2-Diphenyl-2-(p-tolylimino)-1-ethanone. In addition, theoretical study preforms to predict the chemical reactivity and stability of the prepared complexes. Thus, the density function theory (DFT) studies, quantum chemical descriptors like chemical hardness (η), electronic chemical potential (μ), and electronegativity (χ) are considered. Complexes were synthesized in a simple one-pot reaction and chemical structures confirmed by different analysis techniques such as Mass spectra, FT-IR, UV-Vis spectroscopies and thermo gravimetric analysis (TGA). The prepared complexes showed high level of thermal stability according to analysis results as the melting point of the complexes ranged (249-251 ºC).

Keywords: Metal complexes, Schiff base, Syntheses, Thermal analysis, Theoretical studies.

Introduction

Schiff base metal complexes have been studied extensively.[1-3] Even though, Schiff base still attract significant attention. Also, a large number of scientific papers reported every year about its' metal complexes.[4-7] This interest because of tunable properties, cost effective and simple preparation methods that include condensation reaction between primary amine and carbonyl compound.[8-11] Over the past years, Schiff bases transition metal complexes have been utilised in a wide range of applications. For example, in biology Schiff base is used as antibacterial, antifungal, anticancer, antioxidant, anti-inflammatory, antimalarial, antiviral activity.[12-15] Nevertheless, the limited solubility of Schiff base is the main disadvantage that is hard to overcome for this ligand system.[16] Thus, the need to update this ligand system and make it more soluble become more necessary by adding another functional group.[17-20] Current bifunctional ligand system that includes imino and ketone represent an ideal environment for wide range of coordination with different metal centers. Moreover, it has great solubility in the most common solvents. This kind of conjugated is very rare in coordination chemistry. According to our literature review, we did not find previous studies reporting such metal complexes. Herein, we report four new imino-keto complexes and one can say there are no metal complexes

2024, 21(12): 3661-3672
https://doi.org/10.21123/bsj.2024.9852
P-ISSN: 2078-8665 - E-ISSN: 2411-7986
Baghdad Science Journal

reported with this unique imino ethanaone ligand. A theoretical study combined with the structure characterization conducted to evaluate the chemical reactivity of the prepared compounds and to predict the possible reactivity, which include some theoretical determinations such as the DFT, quantum chemical descriptors such a chemical hardness (η), electronic chemical potential (μ), and electronegativity (χ). These descriptors are important to explain the reactivity and stability of studied compounds.[21-24]

The aim of this study is to have deeper insight about these imino-keto complexes and to understand the nature of chemical interactions in order to explore chemical molecules reactivity, atoms, and ions.

Materials and Methods

Chemicals

The analytical grades of 1,2-diphenylethane-1,2-dione (Benzil) and 4-methylaniline (*p*-toluidine) were requested from the common chemical supply (Sigma Aldrich) and used as it received without any further characterization or purification. The FT-IR (Fourier-transform infrared spectroscopy) of were collected for the prepared title compounds on (Bruker) FT-IR Spectrometer from 4000-400 cm^{-1} at 25°C using KBr plates. The ultraviolet-visible spectroscopy (UV-Vis) was recorded for the synthesized compounds in ethanol $1*10^{-3}$. Quartz glass cell (10 mm path length) was used on (Perkin Elmer) spectrophotometer. Mass spectra analyses were performed at the Chemical Analysis Lab., at the Department of Chemistry, College of Science, University of Tehran, Iran using Agilent Technology (HP) (Model: 5973 Network Mass Selective Detector). Thermal analyses data was collected using TA instrument (SDT Q600 V20.9 Build 20) using standard 90 □L alumina metal pans under Ar (50 mL min^{-1}) from 25-800 °C (with a ramp of 10 C min^{-1}). Melting points were determined in glass capillaries.

Ligand Syntheses

Ligands (1,2-Diphenyl-2-(phenylimino)-1-ethanone or 1,2-Diphenyl-2-(*p*-tolylimino)-1-ethanone) were synthesized by adding gradually aniline or 4-methylaniline (1 mmol, 0.09 g or 0.10 g) that is dissolved in 10 mL methanol to round bottom 50 mL charged with 1,2-diphenylethane-1,2-dione (1 mmol, 0.210 g) dissolved in 20 mL methanol. The mixture subsequently was stirred and refluxed for 2 hrs. Consequently, resulted mixture was left to cool down to room temperature. Eq. 1 illustrates the imino-keto synthesis stoichiometric.[25]

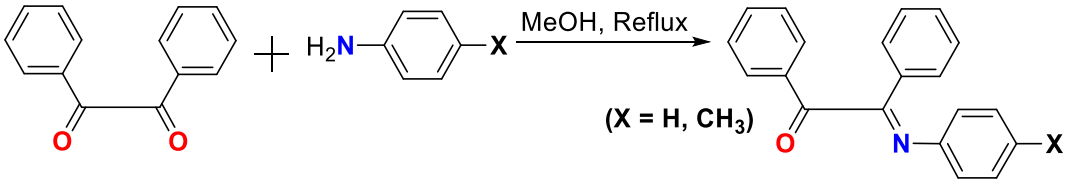

Equation 1.

Complexes Syntheses

Complexation between synthesized ligands (L1, L2) and metals chloride was achieved by adding 10 mL of ethanoic solution of $CoCl_2$ or $CuCl_2$ (1 mmole, 0.12 g, 0.13 g) to (1 mmole, 20 mL) of ligand that charged in a 50 mL round bottom flask Eq. 2. The mixture was stirred and refluxed until the precipitate is formed (2 hours). Reaction was probed by TLC to monitor the progress of reaction mixture. The final product was collected as a white precipitate by filtration. Cold EtOH was employed to remove unreacted chemicals by wash the product several times.

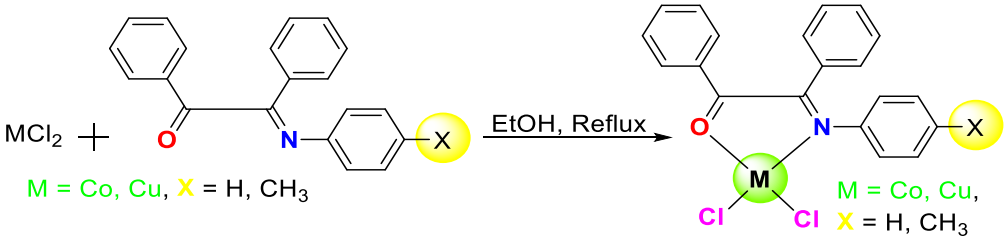

Equation 2.

2024, 21(12): 3661-3672
https://doi.org/10.21123/bsj.2024.9852
P-ISSN: 2078-8665 - E-ISSN: 2411-7986
Baghdad Science Journal

Theoretical Studies

All computational studies and mathematical calculations were collected by the Gaussian 09W program packages using personal computer (Huawei, Core i5, Windows 10).[26] The most common three parameters of Becke's (hybrid functional) that rely on the LYP correlation functional (B3LYP). 6.31G (d, p) basis set combined with the most robust functional of the hybrid family, was employed for theoretical calculations. [27, 28] GAUSSIAN VIEW 05 was utilized to display the collected files from Gaussian program.[29]

Results and discussion

Complex [MCl_2L1] {M = Co (1), M = Cu (2)}

A simple and direct one pot reaction between MCl_2 (M = Co, Cu) and L1 in 1:1 molar ratio was made using ethanol as a solvent Eq. 2, that led to form complex (**1**) in good yield (0.18 g, 85 %, m.p. 243-245 ^oC) and complex (**2**) in good yield also (0.18 g, 85 %, m.p. 241-242 ^oC).

Complex [MCl_2L2] {M = Co (3), M = Cu (4)}

Complexation was achieved for the complexes **3** and **4** by following the same stoichiometry that described above for complexes **1** and **2**. A moderate product yield was collected for complex **3** (0.17 g, 62 %, m.p. 243-245 ^oC) and excellent yield for complex **4** (0.17 g, 62 %, m.p. 249-251 ^oC).

Several spectroscopic techniques (FT-IR, UV, and Mass spectra) have been employed to characterize the prepared iminoketo metal complexes described above Eq. 2. Complexes (**1** and **2**) did not give readable ^{1}H-NMR spectra because of the diamagnetic behavior of copper ion while complexes (**3** and **4**) gave abroad and non-interpret spectra due to paramagnetism nature of cobalt complexes. All the prepared complexes exhibited an excellent level of stability toward wet and air at the ambient temperature (25 ^oC). In addition, complexes (**1-4**) showed a great solubility in ethanol. Thus, chemical structures of all ligands and their complexes confirmed based on a set of accurate chemical and spectroscopic analysis.

FT-IR Spectroscopy

The FT-IR spectra analysis of the complexes (**1-4**) compared with those of the imino ethanaone free ligands L1 and L2 in order to highlight some characteristic peaks of functional groups that may be involved in chelation. In addition, the comparison between the reported vibrational frequencies of the related compounds, such as, the Schiff bases of salicylaldehyde and resacetophenone.[30-33] There are a characteristic peak that used as guide peaks in the spectra of the ligands. Such as the peaks related to azomethine $\tilde{\nu}$ (C= N) and carbonyl $\tilde{\nu}$ (C=O). FT-IR spectra analysis of the imino ethanaone ligands L1 and L2 showed strong bands, at (1650 and 1652) cm^{-1}, and (1695 and 1702) cm^{-1}, assigned to azomethine $\tilde{\nu}$ (C= N) groups and carbonyl groups respectively. These bands confirm the success of ligand synthesis. These results are comparable with the reported studies.[34, 35] A large number of previous studies [32, 33] reported decrease or increase in IR frequencies as a common behaviour in coordination chemistry. For example, the complexation between the metal ions and the azomethine group and carbonyl group with a symmetric phenyl ring shift to higher frequencies. In addition, the electronic density over the metal ion and the bonds can also affect the position of the related peaks toward higher or lower values.[31, 34] IR spectra chart of compounds **1**, **2, 3** and **4** also showed the appearance of sharp peaks at 1449-1593 cm^{-1} these band attributed to carbonyl stretching (C=O) group. Other characteristic bands at the region 1800-2500 cm^{-1} can be recognized for the $\tilde{\nu}$ (C-H) aromatic bending of complexes (**1-4**). The strong and sharp bands located at 1643-16677 cm^{-1} attributed to C=C stretching. Moreover, bands with medium intensity at 678-316 cm^{-1} might attribute to $\tilde{\nu}$ (M-N) vibrations. This is another evidence confirmed the complexation between the metal centre and the functional group of the ligand by the nitrogen atom. The strong sharp bands at 873-875 cm^{-1} indicates the presence of H_2O molecules ν (M-H_2O) in the coordination complexes.[35]

[$CoCl_2L1$] (1)

Herein, the observed IR bands in Fig. 1 at $\tilde{\nu}$ equal to: 3316 (w), 3063 (m), 2445 (m), 1995 (w), 1868 (w), 1660 (s), 1588 (s), 1447 (s), 1393 (w), 1319 (m), 1210 (s), 1169 (s), 994 (w), 937 (w), 740 (w), 873 (s), 719 (s), 686 (m), 638 (s), 461 (m). The $\tilde{\nu}$(C=N) at 1697 (s) cm^{-1}.

2024, 21(12): 3661-3672
https://doi.org/10.21123/bsj.2024.9852
P-ISSN: 2078-8665 - E-ISSN: 2411-7986
Baghdad Science Journal

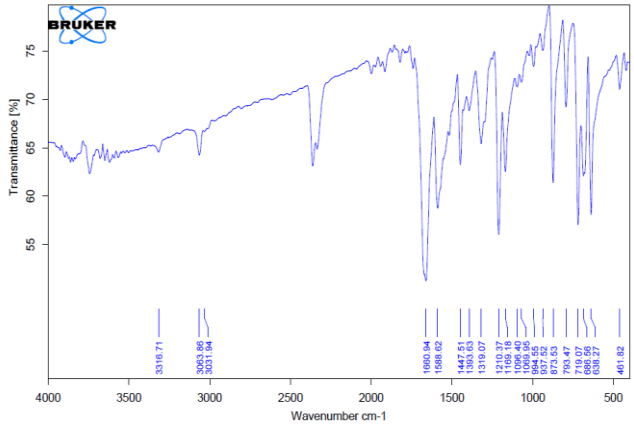

Figure 1. FT-IR spectrum of complex [$CoCl_2L1$] (1).

[$CuCl_2L1$] (2)

Fig. 2. shows a series of bands at $\tilde{\nu}$ equal to: 3316 (w), 3063 (m), 2925 (m), 2000 (w), 1950 (w), 1820 (m), 1659 (s), 1593 (s), 1449 (s), 1324 (m), 1210 (s), 1173 (s), 1097 (s), 1071 (w), 1021 (w), 997 (m), 938 (m), 794 (s), 695 (s), 680 (m), 642 (s), 459 (m) cm^{-1}.

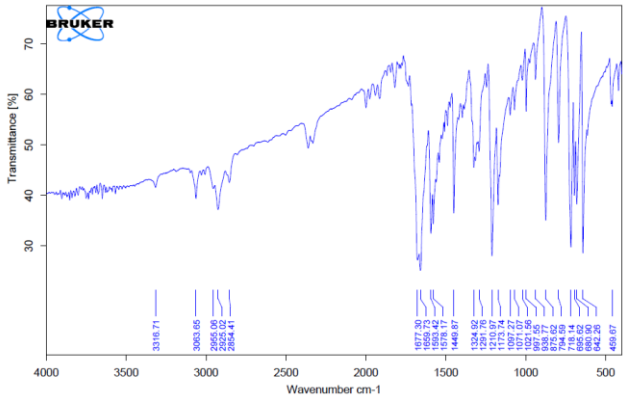

Figure 2. FT-IR spectrum of complex [$CuCl_2L1$] (2).

[$CoCl_2L2$] (3)

The following IR results related to complex 3 showed in Fig. 3 at $\tilde{\nu}$ equal to: 3029 (m), 2435 (w), 2003 (w), 1925 (w), 1885 (m), 1659 (s), 1593 (s), 1489 (w), 1449 (s), 1315 (m), 1210 (s), 1211 (s), 1173 (s), 1097 (m), 1071 (m), 997 (s), 718 (s), 681 (m), 642 (s), 466 (m). The $\tilde{\nu}$(C=N) at 1697 (s) cm^{-1}

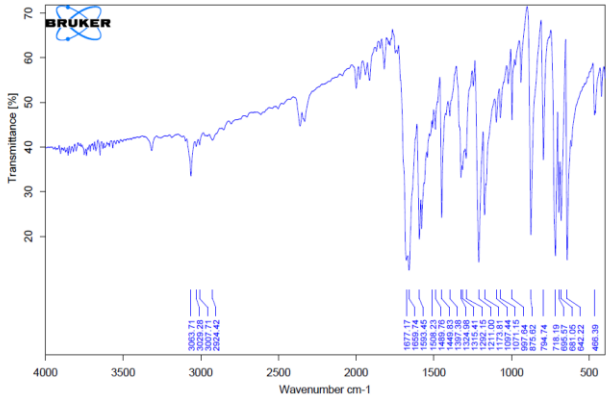

Figure 3. FT-IR spectrum of complex [$CoCl_2L2$] (3).

[$CuCl_2L2$] (4)

The following IR bands were observed in Fig. 4 at $\tilde{\nu}$ equal to: 3064 (m), 2434 (m), 2115 (w), 1930 (w), 1660 (s), 1593 (s), 1578 (s), 1517 (m), 1488 (m), 1449 (s), 1398 (w), 1325 (m), 1211 (s), 1174 (s), 1096 (w), 1072 (w), 1022 (w), 875 (s), 800 (s), 718 (s), 681 (m), 642 (s), 483 (s) cm^{-1}.

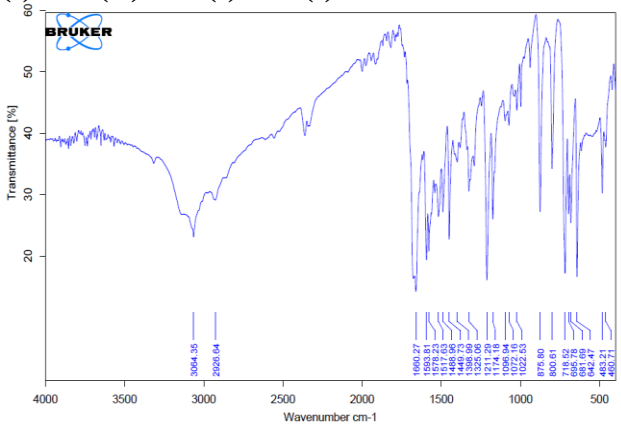

Figure 4. FT-IR spectrum of complex [$CuCl_2L2$] (4).

UV-Visible spectroscopy

UV spectroscopy measurements have employed as a qualitative analysis for the prepared complexes (1-4). In this study, the UV spectroscopic characterizations of all complexes (**1-4**) noticed at the far UV region (296 to 302 nm). Measurements were investigated at 25 °C. Figs. 5-8 showed UV-Visible of complexes **1-4**. UV-Visible absorption appeared at 302, 298, 296, and 300 nm respectively.

The unconjugated chromophore showed bands related to ($\pi \rightarrow *\pi$) in a range (235-272 nm) but these values can affect shifting to high-range depending on aryl or alkyl groups because of ($\pi \rightarrow *\pi$) and ($n \rightarrow *\pi$) electrons transfer. Also, various Schiff base compounds showed two absorption peaks at 230 and 310 nm because of ($\pi \rightarrow *\pi$) electrons transfer and the

2024, 21(12): 3661-3672
https://doi.org/10.21123/bsj.2024.9852
P-ISSN: 2078-8665 - E-ISSN: 2411-7986
Baghdad Science Journal

second peak can appear at 315-375 nm because of (n→*π) electrons' transfer.

[$CoCl_2L1$] (1)

The UV-Vis spectra of the complex **(1),** Fig. 5 displayed a band at 295 nm related to the electronic *π*-transition in the phenyl groups. The band appeared at 215 nm because of the *n*-transition that assigned to the nonbonding electrons present on the nitrogen atom of the azomethine. Moreover, the spectrum of the complex also shows the d-d transition band at 385 nm as a low intensity.

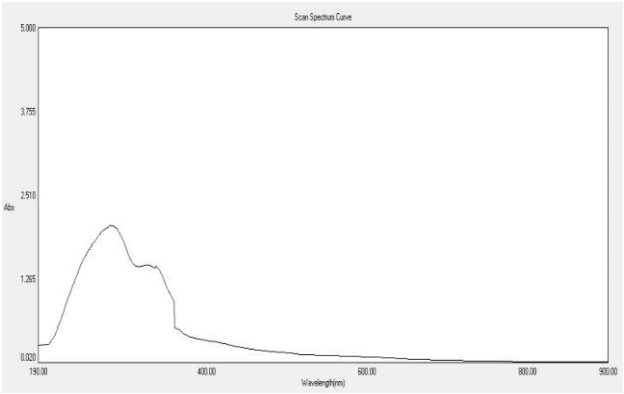

Figure 5. UV-Spectrum of complex [$CoCl_2L1$].

[$CuCl_2L1$] (2)

Fig. 6 showed two different bands at 315 nm due to intraligand transition corresponding to complex (**2**) and the second absorption band with low intensity at 372nm due to (d-d) electronic transition.

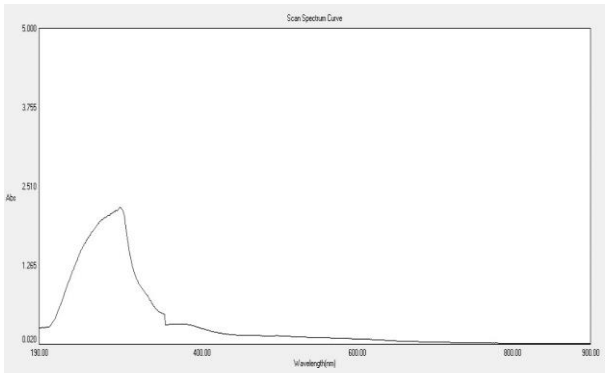

Figure 6. UV-Spectrum of complex [$CuCl_2L1$].

[$CoCl_2L2$] (3)

Electronic data presented in Fig. 7 as strong two bands at 249 nm and 327 nm related to complex **3**. These bands moved towards longer wavelength in comparison with the reported absorptions corresponding to the Schiff base ligand. The first band at 249 nm because of the intraligand electronic transition, while the band at 327 nm because of the charge transfer.

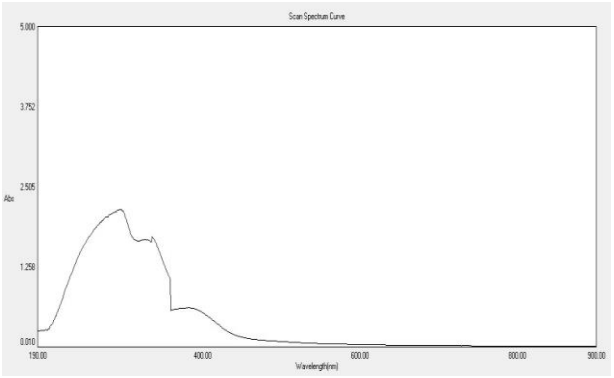

Figure 7. UV-Spectrum of complex [$CoCl_2L2$].

[$CuCl_2L2$] (4)

The electronic spectrum, Fig. 8, of Cu (II) complex showed two bands at 250 nm and 325 nm. The band at 250 nm might attribute to the electronic intraligand transition. However, the second absorption band at 325 nm is due to the charge transfer. According to these transitions, in addition to the results of the spectroscopic analysis such as IR, mass spectra and thermal analysis, we can suggest that an octahedral geometry around the metal ions of the complexes (**1-4**).

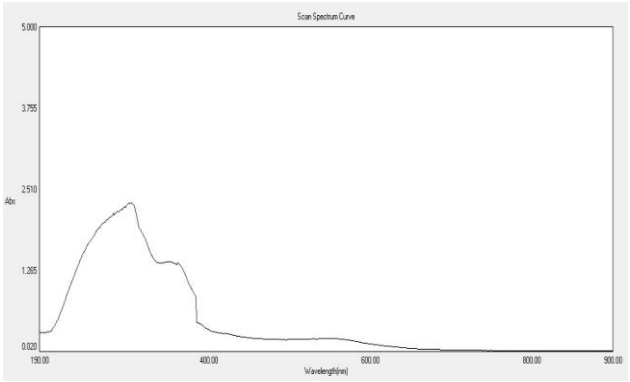

Figure 8. UV-Spectrum of complex [$CuCl_2L2$].

Mass Spectra

The mass spectra were record by exposing all complexes (**1**, **2, 3,** and **4)** to 70 V cone voltages. This amount of voltage can reduce the dissociation of ligand. There is some variation in the isotopes of elements. These differences in the isotopic abundance lead to appear some fragments at higher molecular weight than the calculated. The frequency of the voltage and the steric bulk of the substitution groups also can increase the intensities of peaks.[36] It is hard to avoid water association in such reaction because the water molecules involved in EtOH and

2024, 21(12): 3661-3672
https://doi.org/10.21123/bsj.2024.9852
P-ISSN: 2078-8665 - E-ISSN: 2411-7986
Baghdad Science Journal

MeOH. Thus, some water molecules being coordinated to the metal ions. In such cases, results such as mass spectra must be justified.[37]. Figs. 9-12 summarize the mass spectra of complexes [$CoCl_2L1$] **(1)**, [$CuCl_2L1$] **(2)**, [$CoCl_2L2$] **(3)**, and [$CuCl_2L2$] **(4)** respectively. The spectra showed disappearance of the peak of the molecular ion (M+) due to voltage instability. This situation happened in some instruments and effect on the resolution of the spectra but still some characteristic peaks can be highlighted such as [Co(MeCO-C=NPh+)] that observed at 210 m/z of the [$CoCl_2L1$] **(1)** spectra and [Cu(PhCO-C=NPh+)] at 279 m/z of [$CuCl_2L1$] **(2)**. The spectrum of [$CoCl_2L1$] **(3)** shows a main peak at 299 m/z belongs to [Co(PhCO-C=NPh+)]. An intense peak observed at 279 m/z is due to [Cu(PhCO-C=NPh+)] of [$CuCl_2L1$] **(4)** as described below in Table 1.

Table 1. Mass spectra data of the important mass peak for the complexes (1-4).

Complexes	Mass assignments	M/Z
Complex [$CoCl_2L1$]	[Co(MeCO-C=NPh+)]	210
Complex [$CuCl_2L1$]	[Cu(PhCO-C=NPh+)]	279
Complex [$CoCl_2L2$]	[Co(PhCO-C=NPh+)]	299
Complex [$CuCl_2L2$]	[Cu(PhCO-C=NPh+)]	279

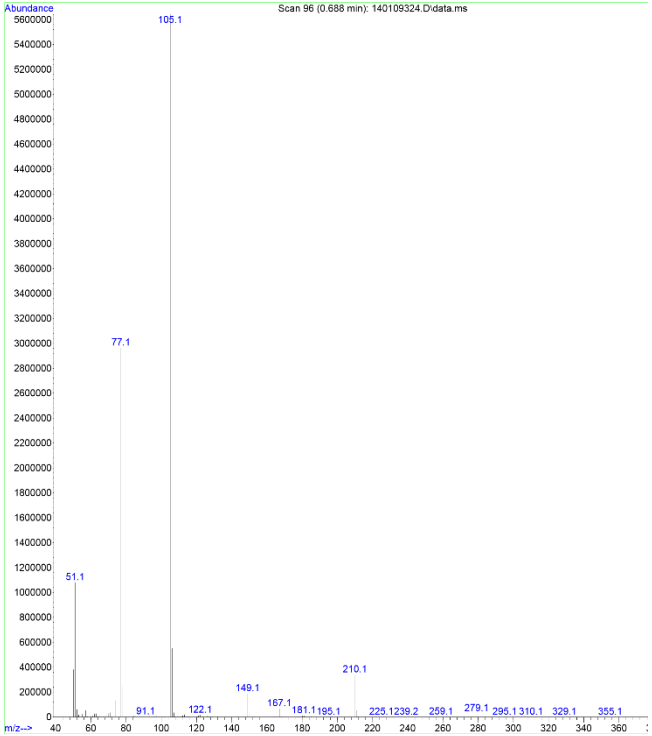

Figure 9. Mass spectrum of [$CoCl_2L1$] complex.

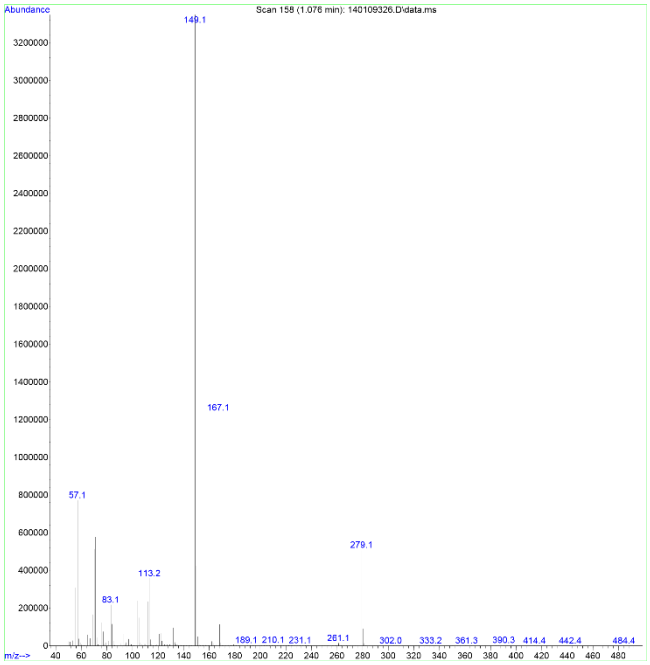

Figure 10. Mass spectrum of [$CuCl_2L1$].

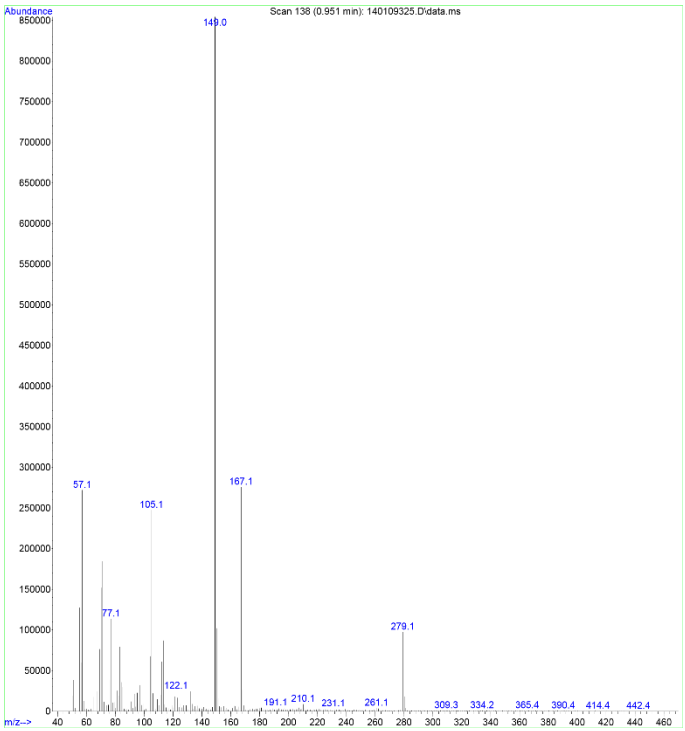

Figure 11. Mass spectrum of [$CoCl_2L2$].

2024, 21(12): 3661-3672
https://doi.org/10.21123/bsj.2024.9852
P-ISSN: 2078-8665 - E-ISSN: 2411-7986
Baghdad Science Journal

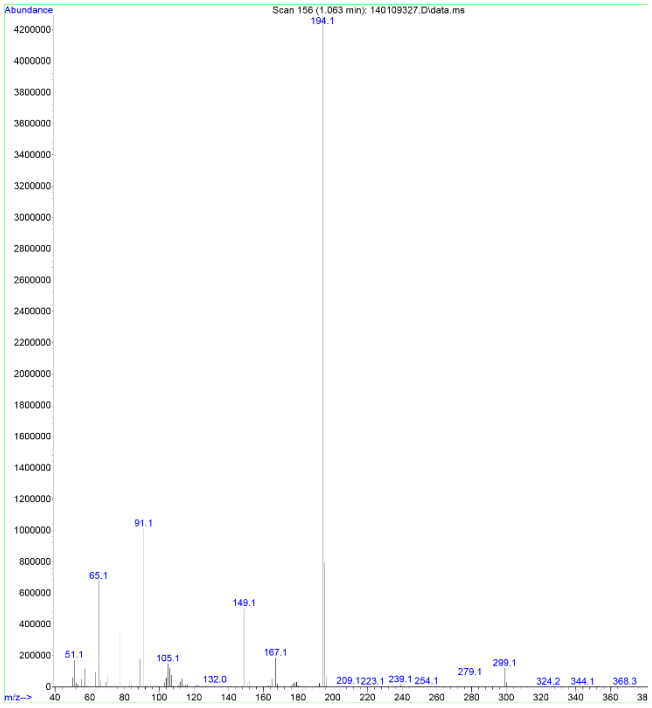

Figure 12. Mass spectrum of [$CuCl_2L2$].

Thermal Analysis

The TGA and DTG studies performed to highlight the thermal behavior of the complexes (**1-4**) and to explore the intermediates fragments and the final products formed because of the thermolysis. The thermal decomposition process of the metal complexes involves generally three consecutive stages (dehydration, ligand pyrolysis and inorganic residues). Figs. 13-16 showed the thermal analysis of complexes (1-4) respectively.[38, 39]

[$CoCl_2L1$] (1)

The TG curve Fig. 13 shows two stages of mass loses which mean the decomposition was continuously. The first peak at 225 ^oC indicating the thermally stability of the compound is up to 225 ^oC. Next stage (225-410 ^oC), the thermal curve showed a mass loss up to 75% as some water molecules eliminated because of the dehydration process.

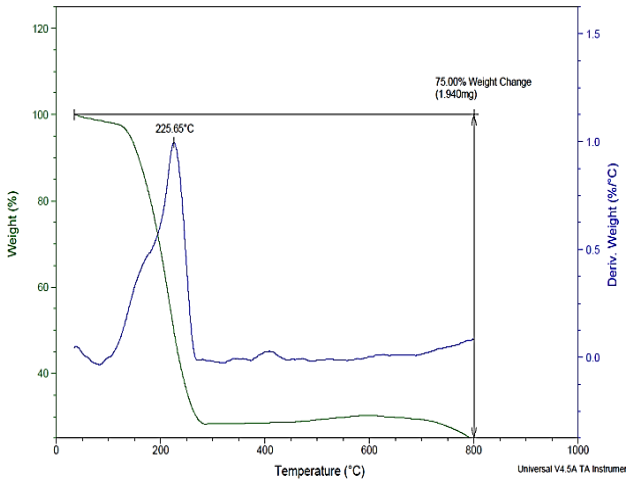

Figure 13. TGA plots of the [$CoCl_2L1$].

[$CuCl_2L1$] (2)

TGA and DTG curves of the bulk sample, Fig. 14, showed only one stage of decomposition as a one peak correspond to DTG at 253.33 ^oC as a result the intermediate compounds did not detected. TG showed a change in the slope at mass loss of 86.04%.

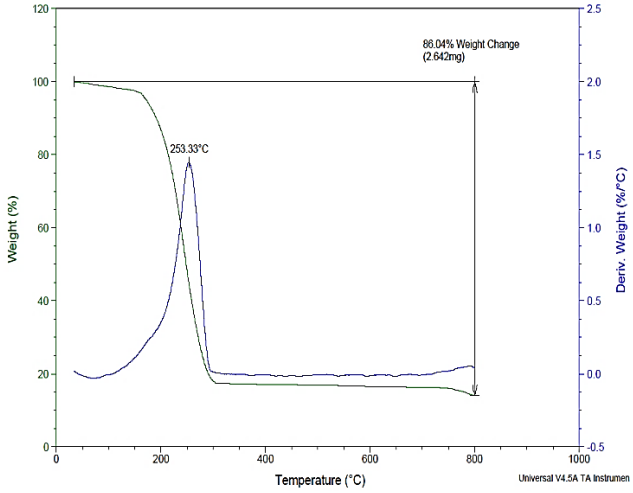

Figure 14. TGA plots of the [$CuCl_2L1$].

[$CoCl_2L2$] (3)

The thermogram showed two, Fig. 15, thermal decomposition patterns. The first stage at 229 ^oC is due to the dehydration of some water molecules. The resulting compound follow DTG plateau up to 380 ^oC after which the curve exhibits a mass loss of 70%.

2024, 21(12): 3661-3672
https://doi.org/10.21123/bsj.2024.9852
P-ISSN: 2078-8665 - E-ISSN: 2411-7986
Baghdad Science Journal

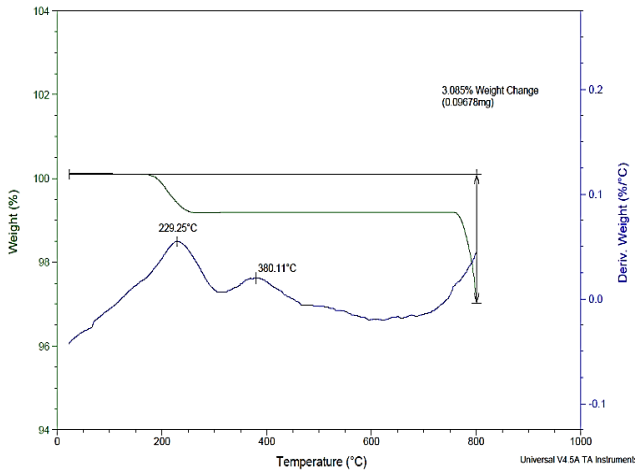

Figure 15. TGA plots of the [$CoCl_2L2$].

[$CuCl_2L2$] (4)

The thermo-analytical curve (TGA curve), Fig. 16, revealed that the title compound undergoes a two decomposition stages. It is interesting to note that the mass loss of the compound remains constant up to a temperature of 260 °C thereafter the first stage started at 261.88 °C. This is confirm the dehydration stage for the complex by eliminating coordinated water molecules. Later the compound experienced a mass loss of about 387.66 °C.

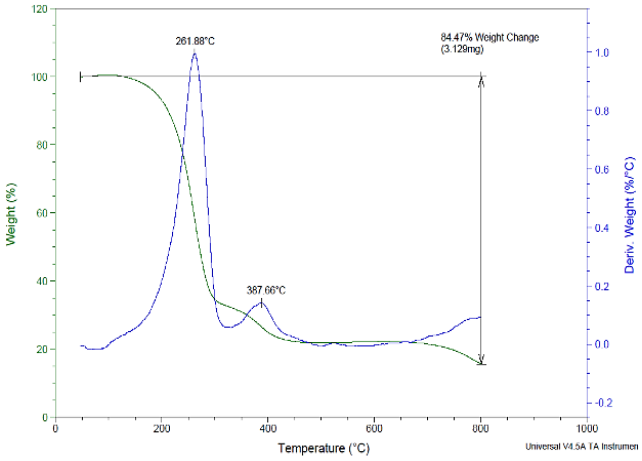

Figure 16. TGA plots of the [$CuCl_2L2$].

Computational Simulation

Theoretical calculations performed in order to investigate the electronic properties and global reactivity parameters of the studied complexes. The electronic properties includes HOMO, LUMO and energy gap (Eg) and the reactivity parameters includes Electronegativity (c), ionization potential (IP), electron affinity (EA), chemical potential (μ), global hardness (η) and global softness (ς). Figs. 17-20 present the optimized geometry while Tables. 2 and 3 present the calculated electronic properties and global reactivity parameters for studied complexes.

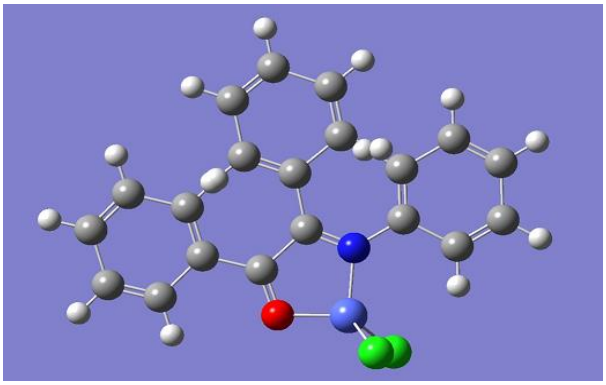

Figure 17. Optimized geometry of the [$CoCl_2L1$].

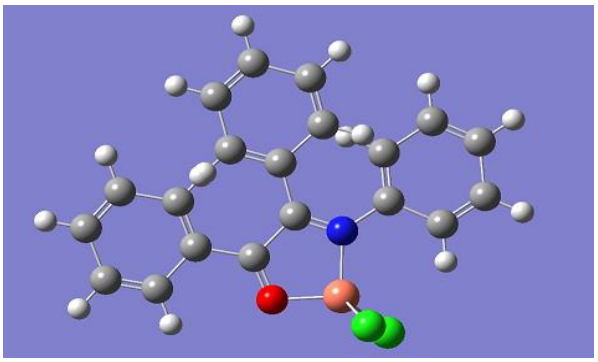

Figure 18. Optimized geometry of the [$CuCl_2L1$].

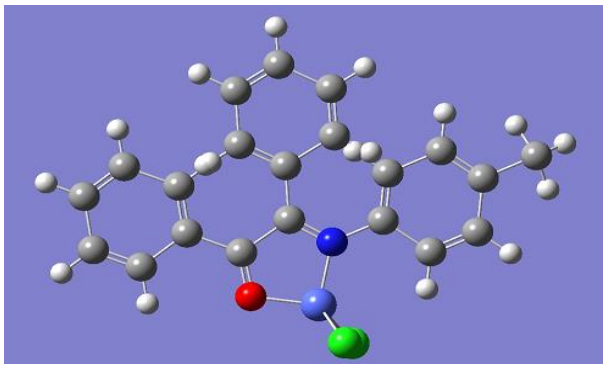

Figure 19. Optimized geometry of the [$CoCl_2L2$].

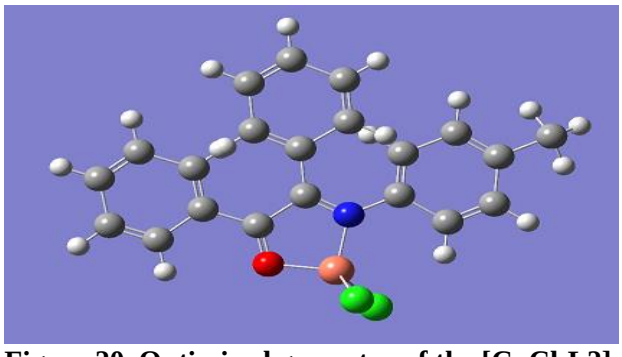

Figure 20. Optimized geometry of the [$CuCl_2L2$].

2024, 21(12): 3661-3672
https://doi.org/10.21123/bsj.2024.9852
P-ISSN: 2078-8665 - E-ISSN: 2411-7986
Baghdad Science Journal

Table 2. HOMO, LUMO and Energy gap values of complex 1.

Model	HOMO ev	HUMO ev	Eg (ev)
Complex [$CoCl_2L1$]	-5.23049842	-5.069137	0.1614
Complex [$CuCl_2L1$]	-4.5578425	-4.511312	0.0465
Complex [$CoCl_2L2$]	-5.69362964	-5.508595	0.185
Complex [$CuCl_2L2$]	-4.60355698	-4.546142	0.0574

Table 3. Reactivity parameters values of complex 1

Model	IP	EA	χ	η	ς	μ
Complex [$CoCl_2L1$]	5.23	5.069	5.15	0.081	6.197	-5.15
Complex [$CuCl_2L1$]	4.558	4.511	4.535	0.023	21.49	-4.535
Complex [$CoCl_2L2$]	5.694	5.509	5.601	0.093	5.404	-5.601
Complex [$CuCl_2L2$]	4.604	4.546	4.575	0.029	17.42	-4.575

From theoretical calculations, it was found that the [$CoCl_2L2$**]** has the lowest energetic gap (Eg = 0.0182 eV), so it is the softest complex and it is the best to be easily excited while the [$CuCl_2L2$] has the highest energy gap (Eg = 0.8661 eV), so it is the hardest molecule.

[$CuCl_2L1$] has the highest HOMO energy (E_{HOMO} = -4.5578425 eV) that allows him to be the best electron donor complex; on the other hand the [$CoCl_2L2$] has the lowest LUMO energy (E_{LUMO} = -5.94369873 eV) that allows it to be the best electron acceptor complex.

The ionization potential (I) and electron affinity (A) depict the electron exchange that involves electron donating/accepting ability of the complexes, respectively.[40] From Table. 3, the [**$CuCl_2L1$**] and complex [**$CuCl_2L1$**] display the lowest ionization potential values therefore showed high electron-donating ability. The electron acceptor or donor properties can also explained in term of electronegativity (χ), which representing the capability of molecules for electrons attraction.[41] Results indicate the complex **[$CuCl_2L2$]** display the highest electronegativity value and high electron acceptor complex while the complex [**$CuCl_2L1$**] show the lowest electronegativity value and high electron donating complex.

The energy gap (E_g) and the hardness (η) of the complex follow the same trend. Complexes with low E_g and η possess low stability and more reactivity. Results indicate that the complex **[$CoCl_2L2$]** has the lowest hardness value (0.009 eV) and more reactive than the other complexes. Global softness (ς) and global hardness (η) follows a reversed trend. Hence, the complex **[$CoCl_2L2$]** has the highest values of the chemical softness (54.85 eV) which expected to show less stability and highest reactivity.

The electronic chemical potential (μ) value gives an idea about the charge transfer within any compound in its ground state. From the results, the complex [**$CuCl_2L1$**] has the highest chemical potential (-4.535 eV) therefore it is less stable and more reactive than the other complexes.

Conclusion

The new prepared iminoketo metal complexes (**1-4**) are characterized by a set of accurate spectroscopic techniques. Such as FT-IR, UV-Vis, mass spectra and thermo gravimetric analysis (TGA). Complexes (**1-4**) were synthesized by reacting the bidentate ligands Eq. 2 with different salts (metal chlorides). Highly air and thermal stable metal complexes [$CoCl_2L1$], [$CuCl_2L1$], [$CoCl_2L2$] and [$CuCl_2L2$] as the melting point reached 237-248 ^oC. This is thermal stability represent a promising result as these complexes can be used as a catalyst for different reactions that required elevated temperatures. Complexes (**1**, **2**, **3, 4**) showed high chemical stability in ethanol for at least 72 hrs. Theoretical studies and computational calculations were conducted for the characterized compounds in order to investigate the electronic properties and global reactivity parameters of the studied complexes. Thus, the density function theory (DFT) studies, quantum chemical descriptors like chemical hardness (η), electronic chemical potential (μ), and electronegativity (χ) were investigated. Results indicate the complexes (**1-4**) display interesting electronegativity that will open the door for further chemical reactivities.

Acknowledgment

Authors gratefully acknowledge Al-Shatrah University and University of Thi-Qar for provided some technical support.

Author's Declaration

- Conflicts of Interest: None.
- We hereby confirm that all the Figures and Tables in the manuscript are ours. Furthermore, any Figures and images, that are not ours, have been included with the necessary permission for re-publication, which is attached to the manuscript.
- Ethical Clearance: The project was approved by the local ethical committee at Al-Shatrah University.
- No animal studies are present in the manuscript.
- No human studies are present in the manuscript.
- No potentially identified images or data are present in the manuscript.

Authors' Contributions Statement

S. H. A. and H. T. O. prepared complexes and performed the experimental analysis. S. S. M., performed the computational studies. S. H. A. and S. G. wrote and discussed the results and contributed the final manuscript.

References

1. Khan E, Hanif M, Akhtar MS. Schiff bases and their metal complexes with biologically compatible metal ions; biological importance, recent trends and future hopes. Rev Inorg Chem. 2022; 42(4): 307-325. https://doi.org/10.1515/revic-2021-0034
2. Ali SH, Abd Alredha HM, Abdulhussein HS. Antibiotic activity of new species of schiff base metal complexes. Per Tchê Quím. 2020; 17(35): 837-859. http://dx.doi.org/10.52571/PTQ.v17.n35.2020.71_ALI_pgs_837_859.pdf
3. Majid SA, Mir JM, Jan G, Shalla AH. Schiff base complexes, cancer cell lines, and anticancer evaluation: a review. J Coord Chem. 2022; 75(15-16): 2018-2038. https://doi.org/10.1080/00958972.2022.2131402
4. Sandhu QUA, Pervaiz M, Majid A, Younas U, Saeed Z, Ashraf A, et al. Schiff base metal complexes as anti-inflammatory agents. J Coord Chem. 2023; 76(9-10): 1094-1118. https://doi.org/10.1080/00958972.2023.2226794
5. Al-Shboul TM, El-khateeb M, Obeidat ZH, Ababneh TS, Al-Tarawneh SS, Al Zoubi MS, et al. Synthesis, characterization, computational and biological activity of some Schiff bases and their Fe, Cu and Zn complexes. Inorganics. 2022; 10(8): 112-127. https://doi.org/10.3390/inorganics10080112
6. Oliveri IP, Consiglio G, Munzi G, Failla S. Deaggregation properties and transmetalation studies of a zinc (II) salen-type Schiff-base complex. Dalton Trans. 2022; 51(31): 11859-11867. https://doi.org/10.1039/D2DT01448C
7. Jain S, Rana M, Sultana R, Mehandi R. Schiff base metal complexes as antimicrobial and anticancer agents. Polycycl Aromat Compd. 2023; 43(7): 6351-6406. https://doi.org/10.1080/10406638.2022.2117210
8. Abd Al-Redha HM, Ali SH, Mohammed SS. Syntheses, structures and biological activity of some schiff base metal complexes. Baghdad Sci J. 2021; 19(3): 704-715. https://doi.org/10.21123/bsj.2022.19.3.0704
9. Skrodzki M, Garrido VO, Csáky AG, Pawluć P. Searching for highly active cobalt catalysts bearing schiff base ligands for markovnikov-selective hydrosilylation of alkynes with tertiary silanes. J Cata. 2022; 411: 116-121. https://doi.org/10.1016/j.jcat.2022.05.002
10. le Roux WH, Matthews M, Lederer A, van Reenen AJ, Malgas-Enus R. First report of schiff-base nickel nanoparticle-catalyzed oligomerization and polymerization of norbornene. J Cata. 2022; 405: 571-587. https://doi.org/10.1016/j.jcat.2021.11.008
11. Białek M, Fryga J, Spaleniak G, Matsko MA, Hajdasz N. Ethylene homo-and copolymerization catalyzed by vanadium, zirconium, and titanium complexes having potentially tridentate schiff base ligands. J Cata. 2021; 400: 184-194. https://doi.org/10.1016/j.jcat.2021.05.036
12. Mondal K, Dey A, Mistri S. Aminoethylpiperazine Based Metal Schiff Base Complexes: Catalytic and Biological Activities. Comm Inorg Chem. 2023; 43(5): 357-381.https://doi.org/10.1080/02603594.2022.2140146

13. Zheng A, Zhou Q, Ding B, Li D, Zhang T, Hou Z. Reduced amino acid schiff base-iron (III) complexes catalyzing oxidation of cyclohexane with hydrogen peroxide. Euro J Inorg Chem. 2021; (33): 3385-3395. https://doi.org/10.1002/ejic.202100356
14. Shekhar S, Khan AM, Sharma S, Sharma B, Sarkar A. Schiff base metallodrugs in antimicrobial and anticancer chemotherapy applications: a comprehensive review. Emerg Mater. 2022; 5(2): 279-293. https://doi.org/10.1007/s42247-021-00234-1
15. Alorini T, Daoud I, Al-Hakimi AN, Alminderej F, Albadri AE. An experimental and theoretical investigation of antimicrobial and anticancer properties of some new Schiff base complexes. Res Chem Intermed. 2023; 49(4): 1701-1730. https://doi.org/10.1007/s11164-022-04922-3
16. Zong LP, Chen X, Zhu D, Li XJ, Li F, Cosnier S, et al. Schiff base complexes with covalently anchored luminophores: self-enhanced electrochemiluminescence detection of neomycin. ACS sensors. 2022; 7(10): 3085-3093. https://doi.org/10.1021/acssensors.2c01425
17. Kanwal A, Parveen B, Ashraf R, Haider N, Ali KG. A review on synthesis and applications of some selected Schiff bases with their transition metal complexes. J Coord Chem. 2022; 75(19-24): 2533-2556. https://doi.org/10.1080/00958972.2022.2138364
18. Yan L, Li Z, Xiong Y, Zhong X, Peng S, Li H. Zinc (ii) Schiff base complexes as dual probes for the detection of NH4+ and HPO4 2− ions. New J Chem. 2022; 46(27): 12910-12917. https://doi.org/10.1039/D2NJ01686A
19. Jain A, De S, Barman P. Microwave-assisted synthesis and notable applications of Schiff-base and metal complexes: a comparative study. Res Chem Intermed. 2022; 48(5): 2199-2251. https://doi.org/10.1007/s11164-022-04708-7
20. Chen YT, Zhang SN, Wang ZF, Wei QM, Zhang SH. Discovery of thirteen cobalt (II) and copper (II) salicylaldehyde Schiff base complexes that induce apoptosis and autophagy in human lung adenocarcinoma A549/DDP cells and that can overcome cisplatin resistance in vitro and in vivo. Dalton Trans. 2022; 51(10): 4068-4078. https://doi.org/10.1039/D1DT03749H
21. Hu F, Yang X, Leng X, Wang C, Yang K, Zhang L, et al. Construction of a near-IR-luminescent rectangular Yb (III) complex from a dodecadentate schiff base ligand for the excitation wavelength dependent detection of aloe emodin (a Natural Medicinal Ingredient). Inorg Chem. 2023; 62(6): 2508-2512. https://doi.org/10.1021/acs.inorgchem.2c04301
22. Wang K, Yang H, Liao Z, Li S, Hambsch M, Fu G, et al. Monolayer assisted surface initiated schiff base mediated aldol polycondensation for the synthesis of crystalline sp2 carbon-conjugated covalent organic framework thin films. J Am. Chem. Soc. 2023; 145(9): 5203-5210. https://doi.org/10.1021/jacs.2c12186
23. Liu SB. Conceptual density functional theory and some recent developments. Acta Physico-Chimica Sinica. 2009; 25(3): 590-600.
24. Frau J, Glossman-Mitnik D. Conceptual DFT descriptors of amino acids with potential corrosion inhibition properties calculated with the latest minnesota density functionals. Front Chem. 2017; 5(16): 1-8. https://doi.org/10.3389/fchem.2017.00016
25. Ali SH, Al-Redha HM, Sachit BA. Antibacterial activity of some salen metal complexes. In IOP Conf Ser.: Mat Sci Eng. 2020; 928(5): 052016. https://doi.org/10.1088/1757-899X/928/5/052016
26. Frisch MJ, Trucks GW, Schlegel HB, Scuseria GE, Robb MA, Cheeseman JR, et al. Gaussian 09, Revision C.01; Gaussian Inc.: Wallingford, CT, USA, 2010.
27. Schlegel HB. Optimization of equilibrium geometries and transition structures. J Comput Chem. 1982; 3(2): 214-218. https://doi.org/10.1002/jcc.540030212
28. Ditchfield R, Hehre WJ, Pople JA. Self-consistent molecular orbital methods. Xii, further extensions of Gaussian-type basis sets for use in molecular orbital studies of organic molecules. J Chem Phys. 1972; 56(5): 2257-2261. https://doi.org/10.1063/1.1677527
29. Dennington R, Keith T, Millam J. Semichem Inc. Shawnee Mission KS, Gauss View, Version. 2009; 5(8): 1-8.
30. Ghosh MK, Pathak S, Ghorai TK. Synthesis of two mononuclear schiff base metal (m= fe, cu) complexes: mof structure, dye degradation, H_2O_2 sensing, and dna binding property. ACS omega. 2019; 4(14): 16068-16079. https://doi.org/10.1021/acsomega.9b02268
31. Garcia-Valle FM, Tabernero V, Cuenca T, Mosquera ME, Cano J. Intramolecular C–F activation in Schiff-base alkali metal complexes. Organometallics. 2019; 38(4): 894-904. https://doi.org/10.1021/acs.organomet.8b00868
32. Klamm BE, Windorff CJ, Celis-Barros C, Marsh ML, Meeker DS, Albrecht-Schmitt TE. Experimental and theoretical comparison of transition-metal and actinide tetravalent schiff base coordination complexes. Inorg Chem. 2018; 57(24): 15389-15398. https://doi.org/10.1021/acs.inorgchem.8b02700
33. Dwivedi N, Sunkari SS, Verma A, Saha S. Molecular packing dependent solid state fluorescence response of supramolecular metal–organic frameworks: phenoxo-bridged trinuclear Zn (II) centered schiff base complexes with halides and pseudohalides. Cryst Growth Des. 2018; 18(9): 5628-5637. https://doi.org/10.1021/acs.cgd.8b00948

2024, 21(12): 3661-3672
https://doi.org/10.21123/bsj.2024.9852
P-ISSN: 2078-8665 - E-ISSN: 2411-7986
Baghdad Science Journal

34. Dong YL, Liu HR, Wang SM, Guan GW, Yang QY. Immobilizing isatin-schiff base complexes in NH2-UiO-66 for highly photocatalytic CO_2 reduction. ACS Catalysis. 2023; 13(4): 2547-2554. https://doi.org/10.1021/acscatal.2c04588
35. Ghosh TK, Maity S, Ghosh S, Gomila RM, Frontera A, Ghosh A. Role of redox-inactive metal ions in modulating the reduction potential of uranyl schiff base complexes: detailed experimental and theoretical studies. Inorg Chem. 2022; 61(18): 7130-7142. https://doi.org/10.1021/acs.inorgchem.2c00645
36. Issa YM, Hassib HB, Abdelaal HE. ^{1}H-NMR, ^{13}C-NMR and Mass spectral studies of some schiff bases derived from 3-amino-1,2,4-triazole. Spectrochimica Acta Part A. 2009; 74: 902-910. https://doi.org/10.1016/j.saa.2009.08.042
37. Irawan C, Islamiyati D, Putri RP, Madiabu MJ. Synthesis and mass spectrum characterization of lyrame schiff base for synthetic ingredients in perfumes industry. Orient J Chem. 2018; 34(6): 3118-3122. https://doi.org/10.13005/OJC%2F340657
38. Rzaczynska Z, Danczowska-Burdon A, Sienkiewicz-Gromiuk J. Thermal and spectroscopic properties of light lanthanides(iii) and sodium complexes of 2, 5-pyridinedicarboxylic acid. J Therm Anal Calor. 2010; 101(2): 671-677. https://doi.org/10.1007/s10973-010-0941-3
39. Caires FJ, Lima LS, Carvalho CT, Giago RJ, Ionashiro M. Thermal behaviour of malonic acid, sodium malonate and its compounds with some bivalent transition metal ions. Thermochimica Acta. 2010; 497: 35-40. https://doi.org/10.1016/j.tca.2009.08.013
40. Obi-Egbedi NO, Ojo ND. Synthesis, light harvesting efciency, photophysical and nonlinear optical properties of 3-(5-(4-hydroxybenzylideneamino) naphthalen-1-yliminomethyl)phenol: Spectroscopic and quantum chemical approach. Res Chem Inter. 2021; 47(12): 5249-5266. https://doi.org/10.1007/s11164-021-04579-4
41. Awolope RO, Ejidike IP, Clayton HS. Schiff base metal complexes as a dual antioxidant and antimicrobial agents. J App Pharma Sci. 2023; 13(3), 132-140. https://doi.org/10.7324/JAPS.2023.91056

تخليق وتشخيص وتحليل حراري ودراسة نظرية لبعض معقدات الايمينوايثانون الفلزية

صفاء حسين علي[1]، سعد شهد محمد[2]، هادي ثامر عبيد[3]، سانجيوا كاماجيدارا[4]

[1] قسم الكيمياء والفسلجة، كلية الطب البيطري، جامعة الشطرة، الشطرة، العراق.
[2] قسم الكيمياء، كلية العلوم، جامعة ذي قار، الناصرية، العراق.
[3] قسم الفيزياء، كلية العلوم التطبيقية، جامعة الشطرة، الشطرة، العراق.
[4] قسم الكيمياء، كلية العلوم، جامعة اوكلاهوما المركزية، اوكلاهوما، الولايات المتحدة.

الخلاصة

الدراسة الحالية صممت لتخليق أربعة معقدات جديدة ثنائية السن من معقدات الايمينوايثانون الفلزية. اذ تضمن التفاعل بين مركبات الايمينوايثانون العضوية كليكاندات واملاح فلزات النحاس والكوبلت (كلوريد النحاس وكلوريد الكوبلت) اذ كانت مركبات الايمينوايثانون تحتوي على معوضات مختلفة على حلقة الفنيل مثل مجموعة المثيل في الموقع بارا. حصل التناسق بين مركز الذرة الفلزية والمجموعات الفعالة على اليكاندات والتي شملت مجاميع (الايزوميثين والايثانون). تضمن البحث كذلك مجموعة من الدراسات النظرية لاستقراء الفعالية الكيميائية والثابتية الحرارية للمعقدات المحضرة شملت دراسات الكثافة الوظيفية وميكانيك الكم الذي بدوره شمل العوامل التالية الصلابة الكيميائية، الاحتمالية الالكترونية الكيميائية، والسالبية الكهربائية. استخدم تفاعل الخطوة الوحدة بين الفلزات والمعقدات لتحضير المعقدات والتي شخصت بدورها من خلال عدد من التقنيات الكيميائية مثل مطيافية الاشعة تحت الحمراء ومطيافية الاشعة فوق البنفسجية والتحلل الحراري وطيف الكتلة لتحديد التركيب الكيميائي الدقيق للمركبات المحضرة ومعقداتها. اثبتت الدراسات الحرارية استقرارية حرارية عالية للمعقدات المحضرة اذ تراوحت درجات انصهار المعقدات المحضرة بين 249-251 ^{o}م.

الكلمات المفتاحية: معقدات فلزية، قواعد شف، تخليق، تحلل حراري، دراسات نظرية.